Defective insulin-stimulated GLUT4 translocation in brown adipocytes induces systemic glucose homeostasis dysregulation independent of thermogenesis in female mice

Belén Picatoste [1], Lucie Yammine [1,4], Rosemary A. Leahey [1,4], David Soares [1], Emma F. Johnson [1], Paul Cohen [2], Timothy E. McGraw [1,3,*]

ABSTRACT

Objective: Recent studies indicate that brown adipose tissue, in addition to its role in thermogenesis, has a role in the regulation of whole-body metabolism. Here we characterize the metabolic effects of deleting Rab10, a protein key for insulin stimulation of glucose uptake into white adipocytes, solely from brown adipocytes.

Methods: We used a murine brown adipocyte cell line and stromal vascular fraction-derived *in vitro* differentiated brown adipocytes to study the role of Rab10 in insulin-stimulated GLUT4 translocation to the plasma membrane and insulin-stimulated glucose uptake. We generated a brown adipocyte-specific Rab10 knockout for *in vivo* studies of metabolism and thermoregulation.

Results: We demonstrate that deletion of Rab10 from brown adipocytes results in a two-fold reduction of insulin-stimulated glucose transport by reducing translocation of the GLUT4 glucose transporter to the plasma membrane, an effect linked to whole-body glucose intolerance and insulin resistance in female mice. This effect on metabolism is independent of the thermogenic function of brown adipocytes, thereby revealing a metabolism-specific role for brown adipocytes in female mice. The reduced glucose uptake induced by Rab10 deletion disrupts ChREBP regulation of de novo lipogenesis (DNL) genes, providing a potential link between DNL in brown adipocytes and whole-body metabolic regulation in female mice. However, deletion of Rab10 from male mice does not induce systemic insulin resistance, although ChREBP regulation is disrupted.

Conclusions: Our studies of Rab10 reveal the role of insulin-regulated glucose transport into brown adipocytes in whole-body metabolic homeostasis of female mice. Importantly, the contribution of brown adipocytes to whole-body metabolic regulation is independent of its role in thermogenesis. It is unclear whether the whole-body metabolic sexual dimorphism is because female mice are permissive to the effects of Rab10 deletion from brown adipocytes or because male mice are resistant to the effect.

1. INTRODUCTION

Insulin-stimulated glucose uptake into fat and muscle is mediated by redistribution of the glucose transporter protein 4 (**GLUT4**) from intracellular storage sites to the plasma membrane [1]. Deletion of the small GTPase, Rab10, from white and brown adipocytes blunts GLUT4 translocation and insulin-stimulated glucose uptake by approximately 50% [2,3]. This partial blunting of insulin-stimulated glucose uptake is sufficient to induce systemic insulin resistance, primarily owing to hepatic insulin resistance [3]. The systemic insulin resistance of adiponectin-CRE-driven adipose Rab10 knockout mice is similar to that of adipose GLUT4 knockout, even though in the latter model, there

is a complete loss of insulin-stimulated glucose uptake into adipocytes [4].

The partial (50%) reduction of insulin-stimulated glucose uptake in adipose Rab10 knockout mice linked to severe blunting of liver insulin sensitivity supports a metabolic sensing role for adipose-glucose metabolism. Although the exact mechanism(s) underlying adipose glucose sensing and its impact on whole-body metabolic regulation have not been defined, expression of the β isoform of carbohydrate responsive-element binding protein (**ChREBPβ**) is affected in both adipose-specific GLUT4 and Rab10 KO knockout mouse models [3,5]. ChREBP is a carbohydrate-activated transcription factor [6], linking its regulation to changes in glucose flux downstream of GLUT4 or Rab10

[1]Department of Biochemistry, Weill Cornell Medical College, New York, NY, 10065, USA [2]Laboratory of Molecular Metabolism, The Rockefeller University, New York, NY, 10065, USA [3]Department of Cardiothoracic Surgery, Weill Cornell Medical College, New York, NY, 10065, USA

[4] Lucie Yammine and Rosemary A. Leahey contributed equally to this work.

*Corresponding author. Department of Biochemistry, Weill Cornell Medical College, New York, NY, 10065, USA. E-mail: temcgraw@med.cornell.edu (T.E. McGraw).

Original Article

knockout. Reinforcing the link between adipose ChREBP and whole-body metabolic regulation, adipose knockout of ChREBP is associated with systemic insulin resistance [7].

Previous studies documenting the role of adipose glucose metabolism in the control of whole-body metabolism relied on adiponectin-Cre to generate conditional knockout mice [3,4]. Because adiponectin is expressed by both white and brown adipocytes, the insulin-resistant phenotypes could be caused by changes in white, brown, or both types of adipocytes. Brown adipose tissue (**BAT**) has mainly been described as a thermoregulatory organ, but recent studies document a role for BAT in expanding energy and in the regulation of metabolism [8–11]. Notably, insulin stimulates glucose uptake into BAT [12] and radiolabeled glucose accumulation in BAT is reduced in insulin-resistant individuals, supporting a direct role for BAT in postprandial glucose homeostasis [13].

Here, we demonstrate the role of Rab10 in insulin-stimulated GLUT4 translocation and glucose uptake by brown adipocytes. Silencing Rab10 in brown adipocytes of female mice results in glucose intolerance and insulin resistance, without an effect on BAT thermogenesis. ChREBPβ expression is reduced in BAT of brown adipocyte knockout (**bR10KO**) mice, linking the whole-body metabolic phenotype to ChREBP-dependent glucose sensing in female brown mice. There was no whole-body metabolic phenotype in male bR10KO mice, despite a reduction of ChREBPβ expression in BAT. Thus, either female mice are permissive to the effect of BAT Rab10 knockout or male mice are dominant to it.

2. MATERIAL AND METHODS

2.1. Experimental models and animal details

2.1.1. Brown adipose tissue-specific Rab10 knockout mice
Adipose-specific Rab10KO mice (**aR10KO**) were generated as previously published by our group [3]. We used mice with C57BL/6J genetic background. Cre-lox recombination was used to generate the BAT-specific Rab10KO mice (bR10KO). Mice with loxP sites flanking exon 1 of Rab10 were bred with UCP-1-cre transgenic mice [14,15] to specifically delete Rab10 from mature adipocytes expressing UCP1. Heterozygotes with (Rab10$^{fl/wt}$ + cre) and without (Rab10$^{fl/wt}$) the UCP1-cre transgene were bred to generate mice for further breeding. Homozygote flox females (Rab10$^{fl/fl}$ + cre) and homozygote (Rab10$^{fl/fl}$) were bred to generate mice for the experiments. Control data were derived from Rab10$^{fl/fl}$ littermate mice. Mice were maintained on a standard 12-h light/dark cycle and had *ad libitum* access to water and food. Mice were fed a standard rodent chow diet (5053, PicoLab® Rodent Diet) or 60% irradiated high-fat diet (D12492, Research Diets). Animals were handled in accordance with guidelines of the Weill Cornell Medicine Institutional Animal Care and Use Committees.

2.1.2. Genotyping
Toe or tail DNA was retrieved through digestion with 50 mM NaOH and Tris and was used in touchdown PCR. Cre and IRS recombination was verified by using the following primers: CRE (5′-ATGTCCAATTTACT-GACC-3′ and 3′-CGCCGCATAACCAGTGAAAC-5′) and IRS (5′-GTCTTGCTCAGCCTCGCTAT -3′ and 3′- ACAGCGTGAATTTTGGAGTCA-GAA-5′). Rab10 recombination was verified by using the following pair of primers: Rab10 (5′ —GGTAAAGGCAAGTAGATGTCCATG and 3′ — GAAGAGCAATTAAACACTGCATGC).

2.1.3. Cell lines and culture
Immortalized murine prebrown adipocytes (HBA cells [16], were cultured in Dulbecco's Modified Eagle's Medium - high glucose (D5796, Sigma—Aldrich) supplemented with 20% FBS (26140-095, Life Technologies), and penicillin/streptomycin (15070-063, Life Technologies) at 37 °C/5% CO$_2$. HBA cells were isolated from the fibro-stromal vascular fraction of the intercapular brown fat immortalized with SV 40 T antigen [16,17]. To generate the stable Rab10 KD prebrown adipocyte cell line, we used pSIREN RetroQ system from Clontech, encoding sequences that target Rab10 [2].

For differentiation, parental HBA and Rab10 KO HBA cells were plated at approximately 60—80% confluence and differentiated with growth media containing 20 nM insulin (I5500, Sigma—Aldrich) and 1 nM T3 (T5516, Sigma—Aldrich). On the third day following plating, cells were induced with growth media containing 20 nM insulin, 5.1 μM dexamethasone (D4902, Sigma—Aldrich), 0.5 mM IBMX (I5879, Sigma—Aldrich), and 0.125 mM indomethacin (I7378, Sigma—Aldrich). After one day, the induction media were replaced with growth media containing 20 nM insulin. Experiments were performed 2 days later. HBA cells are sensitive to adrenergic and insulin stimulation, and they have been used in several studies as a cultured brown fat cell model [16–21].

The stromal vascular fraction (SVF) was isolated from digested BAT (digestion buffer: 125 mM NaCl, 5 mM KCl, 1.3 mM CaCl$_2$, 5 mM glucose 1% pen/strep, 100 mM HEPES, 4% BSA, and 1.5 mg/mL Collagenase B) and cultured in DMEM/F12 GlutaMAX (1X) media (10565018, Gibco) containing 10% FBS and 1% pen/strep. Upon confluence, cells were differentiated in DMEM/F12 media containing 10% FBS, 1 μM rosiglitazone, 1 μM dexamethasone, 0.5 mM IBMX, 17 nM insulin, 1 nM T3 (day 0), and 1 μM rosiglitazone. After 2 days, SVF adipocytes were maintained in media containing 10% FBS, 17 nM insulin, and 1 μM rosiglitazone. Two days later, rosiglitazone was removed, but 17 nM insulin was continued. Experiments were performed on day 6 after differentiation.

2.2. Method details

2.2.1. Glucose uptake in murine brown adipocytes and brown adipose tissue stromal vascular fraction adipocytes
For glucose uptake experiments, cells were starved for 1 h. Then cells were incubated in prewarmed 0.1% BSA KRP buffer (1.2 M NaCl, 48 mM KCl, 12 mM KH$_2$PO$_4$, 6 mM MgSO$_4$(H$_2$O)$_7$, 12 mM CaCl$_2$, 20 mM HEPES, 100 nM adenosine and 2.5% insulin and fatty acids-free BSA) for 1 h. Cells were incubated with 10 nM insulin for 20 min before glucose stimulation for 10 min (^{3}H-2-deoxyglucose (50 nM; NET549250UC, PerkinElmer) and diluted in nonradioactive glucose. Cells were washed with PBS and lysed with 0.1% Triton solution. Samples were transferred to vials containing scintillation fluid for radioactivity measurement in a scintillation counter. Glucose uptake was normalized to protein concentration.

2.2.2. GLUT4 translocation assay in murine brown adipocytes
For GLUT4 translocation experiments, immortalized murine brown adipocytes derived from previously characterized immortalized pre-brown adipocytes [16] were differentiated as described in previous sections. Differentiated brown adipocytes were electroporated with 45 μg of HA-GLUT4-GFP. The next day, the brown adipocytes were serum-starved for 2 h and insulin was applied for 30 min. Cells were

fixed with 3.7% formaldehyde for 6 min and GLUT4 on the cell surface was detected by an anti-HA antibody (1:1,000; MMS-101, BioLegend) without permeabilization. HA staining was visualized with Cy3-goat-antimouse (111-165-062, Jackson Immunoresearch). The surface HA signal was normalized to the GFP signal (total GLUT4). Perilipin, as an adipocyte differentiation marker, was assessed using perilipin antibody (1:300; 9349, Cell Signaling Technology).

2.2.3. Glucose and insulin tolerance tests

For glucose tolerance tests (GTT), mice were fasted for 16 h and acclimated to the procedure room with access to water. Mice were intraperitoneally (IP) injected with 2 g/kg of body weight glucose (G7528-1 KG, Sigma). Blood was collected from the tail using Micro-vette® CB 300 LH Heparin (16443100, SARSTEDT) and glucose levels were measured at 0, 3, 15, 30, 45, and 60 min time points. For the HFD experiments, 90 and 120 min time points were added. Plasma insulin levels were measured at 0, 3, 15, and 30 min after glucose injection. For insulin tolerance tests (ITT), mice were fasted for 5 h and acclimated to the procedure room with access to water. Mice were intraperitoneally (IP) injected with 0.5 unit/kg of body weight insulin for NCD-fed mice or 1 unit/kg of body weight insulin for HFD-fed mice insulin (Humulin R, Lilly), and glucose levels were measured at 0, 3, 15, 30, 45, and 60 min time points.

2.2.4. Diet-induced obesity

For HFD studies, control and bR10KO mice were fed a HFD with 60% fat (D12492, Research Diets) or chow diet (D12450B, Research Diets) for 20 weeks (female mice) or 25 weeks (male mice). The challenge with HFD started at 6 weeks of age. GTT was performed in females after 13 weeks on HFD and in males after 17 weeks on HFD.

2.2.5. Cold-induced thermogenesis and thermoneutrality studies

Cold experiments were performed in an environmentally-controlled chamber with the temperature set at 4 °C. Control and bR10KO mice were individually housed with *ad libitum* access to food and water for 14 days at 4 °C. During this period, core body temperature was measured once a day using a rectal probe attached to a digital thermometer. After 14 days, mice were removed and immediately euthanized for tissue collection. Thermoneutrality experiments were performed at the Metabolic Phenotyping Center at Weill Cornell Medicine. Control and bR10KO mice were housed for 21 days in an environmentally-controlled chamber with the temperature set at 30 °C. At day 19, the animals were subjected to a GTT: mice were fasted for 16 h followed by an IP injection with 2 g/kg of body weight glucose (G7528, Sigma). After 21 days, core body temperature was measured using a rectal probe attached to a digital thermometer. Mice were removed from the chamber and immediately euthanized for tissue collection.

2.2.6. Plasma measurements

Plasma insulin (90082, Crystal Chem, Inc) and nonesterified fatty acids (NEFAs) (HR series, Wako) were measured following manufacturer instructions.

2.2.7. Histology

For staining of adipose tissue for BAT and iWAT, samples were dissected and fixed in 10% neutral buffer formalin overnight at 4 °C. Samples were washed in PBS and processed for paraffin embedding using a TissueTek VIP 150 (8315-30-0016, Sakura) in the Electron Microscopy and Histology Core of Weill Cornell Medicine. Embedded blocks were sectioned at 5 μm thickness by the Laboratory of

Comparative Pathology at Memorial Sloan Kettering. Slides were deparaffinized and stained with hematoxylin and eosin. The sections were imaged on a Zeiss AxioPlan microscope in the Electron Microscopy and Histology Core of Weill Cornell Medicine. Images were captured at 10X and 20X magnifications.

2.2.8. RNA isolation and quantitative real-time polymerase chain reaction (qRT-PCR)

A piece of frozen tissue (BAT, iWAT, and eWAT) was disrupted and homogenized in 1 mL of Qiazol lysis reagent (79306, Qiagen) by using a bead mill homogenizer (Omni International). Samples were placed on the bench at room temperature for 5 min and 0.2 mL of chloroform (C0549-1QT, Sigma) was added to each tube. The samples were vortexed and centrifuged at 12,000 rpm for 15 min. The aqueous phase was transferred in a new tube and mixed with 1 volume of 70% ethanol. The volume was transferred to an RNeasy spin column and the protocol for the RNeasy mini kit (74106, Qiagen) was followed. Amplifications were performed using primers summarized in Supplementary file 1, table 1.

Table 1 — List of foward and reverse primer sequences used for qRT-PCR.

Species	Gene name	Primer
Mouse	HPRT	Forward: TGCTCGAGATGTCATGAAGG
		Reverse: TATGTCCCCCGTTGACTGAT
Mouse	ChREBPα	Forward: CGACACTCACCCACCTCTTC
		Reverse: TTGTTCAGCCGGATCTTGTC
Mouse	ChREBPβ	Forward: TCTGCAGATCGCGTGGAG
		Reverse: CTTGTCCCGGCATAGCAAC
Mouse	Srebp1c	Forward: GGAGCCATGGATTGCACATT
		Reverse: GGCCCGGGAAGTCACTGT
Mouse	Fasn	Forward: GGAGGTGGTGATAGCCGGTAT
		Reverse: TGGGTAATCCATAGAGCCCAG
Mouse	DIO2	Forward: AATTATGCCTCGGAGAAGACCG
		Reverse: GGCAGTTGCCTAGTGAAAGGT
Mouse	ACC1	Forward: GATGAACCATCTCCGTTGGC
		Reverse: GACCCAATTATGAATCGGGAGTG
Mouse	UCP1	Forward: AGGCTTCCAGTACCATTAGGT
		Reverse: CTGAGTGAGGCAAAGCTGATTT
Mouse	Adiponectin	Forward: TGTTCCTCTTAATCCTGCCCA
		Reverse: CCAACCTGCACAAGTTCCCTT
Mouse	PPARγ	Forward: GGAAAGACAACGGACAAATC
		Reverse: TGGACACCATACTTGAGCAG
Mouse	PGC1α	Forward: TATGGAGTGACATAGAGTGTGCT
		Reverse: CCACTTCAATCCACCCAGAAAG
Mouse	CIDEA	Forward: TGACATTCATGGGATTGCAGAC
		Reverse: GGCCAGTTGTGATGACTAAGAC
Mouse	PRDM16	Forward: CCAAGGCAAGGGCGAAGAA
		Reverse: AGTCTGGTGGGATTGGAATGT
Mouse	FABP4	Forward: AAGGTGAAGAGCATCATAACCCT
		Reverse: TCACGCCTTTCATAACACATTCC
Mouse	HSL	Forward: CCAGCCTGAGGGCTTACTG
		Reverse: CTCCATTGACTGTGACATCTCG
Mouse	FABP5	Forward: TGAAAGAGCTAGGAGTAGGACTG
		Reverse: CTCTCGGTTTTGACCGTGATG
Mouse	CPT1b	Forward: GCACACCAGGCAGTAGCTTT
		Reverse: CAGGAGTTGATTCCAGACAGGTA
Mouse	VLCAD	Forward: CTACTGTGCTTCAGGGACAAC
		Reverse: CAAAGGACTTCGATTCTGCCC
Mouse	LCAD	Forward: TCTTTTCCTCGGAGCATGACA
		Reverse: GACCTCTCTACTCACTTCTCCAG
Mouse	SCAD	Forward: TGGCGACGGTTACACACTG
		Reverse: GTAGGCCAGGTAATCCAAGCC
Mouse	ATGL	Forward: GAGACCAAGTGGAACATC
		Reverse: GTAGATGTGAGTGGCGTT
Mouse	Rab10	Forward: GGCAAGACCTGCGTGCCTTTT
		Reverse: GTGATGGTGTGAAATCGCTCC

2.2.9. Protein extraction and western blot analysis

Protein was extracted from the frozen tissues of iWAT, BAT, muscle, and liver by using cell lysis buffer (9803S, Cell Signaling Technology) supplemented with a complete protease and phosphatase inhibitor cocktail (78442, Thermo), and centrifuged at 12,000 rpm for 15 min at 4 °C. The supernatant was collected, and protein concentration was measured using a BCA protein quantification kit (Thermo Scientific, Waltham, MA). Protein of 35 μg was separated from acrylamide gels

and blotted onto nitrocellulose membranes. Membranes were blocked at room temperature for 1 h in 5% milk in Tris-buffered saline-Tween (TBS-T). Membranes were incubated with the following primary antibodies (diluted 1:1000 in a 2% BSA-TBS-T) overnight at 4 °C: anti-actin (AAN01-A, Cytoskeleton), anti-Rab10 (4262, Cell Signaling Technology), anti-fatty acid synthase (3180, Cell Signaling Technology), anti-acetyl-coa carboxylase (3676, Cell Signaling Technology), anti-UCP1 (ab10983, abcam), anti-AKT (2920, Cell Signaling
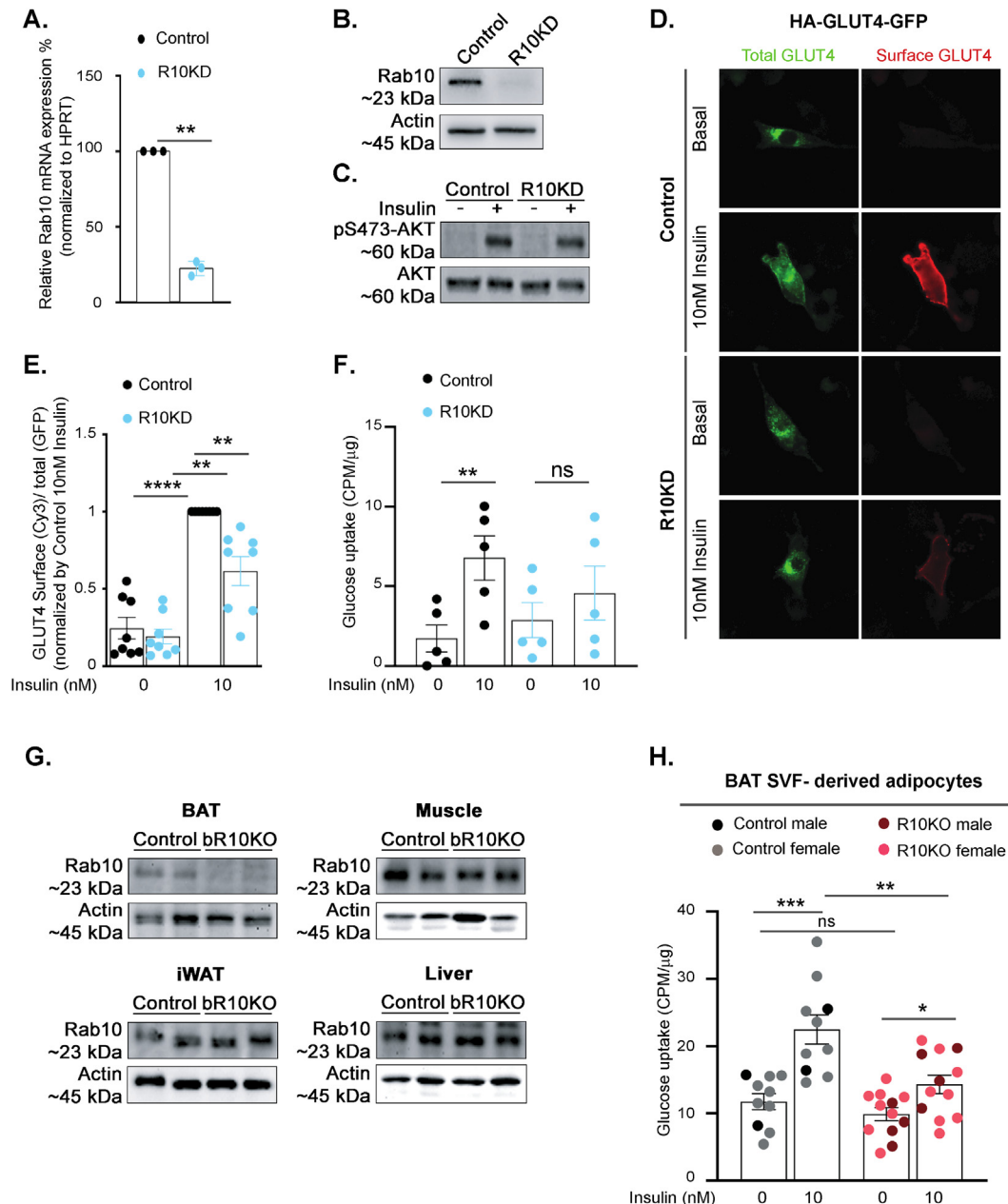
Figure 1: Rab10 deletion impairs insulin-stimulated GLUT4 translocation and glucose uptake in brown adipocytes. A. Rab10 mRNA levels in control and Rab10KD cultured murine brown adipocytes (n = 3). B. Representative Rab10 western blot of protein lysates from control and R10KD cultured brown adipocytes. C. Representative pS473-Akt and total Akt western blot of protein lysates from control and R10KD cultured brown adipocytes. D. Immunofluorescence staining of basal and 10 nM insulin-treated cultured murine brown adipocytes expressing HA-GLUT4-GFP. E. Quantification of the surface-to-total ratio of HA-GLUT4-GFP in cultured murine brown adipocytes. Each symbol is the average value from an independent experiment (n = 8 experiments). In each experiment, 15−50 cells were analyzed per condition. F. Insulin-stimulated glucose uptake (CPM normalized by μg protein) in control and Rab10KD cultured murine brown adipocytes (n = 5 experiments). G. Rab10 representative immunoblots of brown adipose tissue (BAT), inguinal white adipose tissue (iWAT), muscle and liver extracts from control and bR10KO mice. H. Insulin-stimulated glucose uptake (CPM normalized by μg protein) in BAT SVF-derived adipocytes (n = 10−12 mice/group). Data from females are shown in grey and light red dots and data from males are shown in black and dark red dots. Student's t-test was used for comparing groups. *p < 0.05, **p < 0.01, ***p < 0.001, and ****p < 0.0001.

Technology), and anti-phospho-S473-AKT (9271, Cell Signaling Technology). Blots were incubated with goat anti-rabbit IgG-HRP (31460, Thermo Fisher), IRDye® 680LT goat anti-rabbit IgG (102971-010, VWR international) and IRDye® 800CW goat anti-mouse IgG (102971-154, VWR International) for 1 h at room temperature. The blots were developed with the My ECL Imager (Thermo Fisher) and the Odyssey® Fc Imaging system (Li-cor) and quantified with Image J software.

2.2.10. Quantification and statistical analysis
Figure legends indicate all the participant numbers/replicates per study. Results are expressed as means ± SEM. All experiments were repeated at least thrice. At least 3 mice per condition and per genotype were used as biological replicates for *in vivo* experiments. Data were analyzed using Prism 6.0 and Prism 8.0 (GraphPad), ImageJ, and Metamorph software. Groups were compared with an analysis of variance (ANOVA) or a Student's t-test, and a P-value < 0.05 was considered as significantly relevant. All statistical analyses were performed on raw, unnormalized data.

3. RESULTS

3.1. Rab10 silencing blunts insulin-stimulated GLUT4 translocation to the plasma membrane and glucose uptake in brown adipocytes
An immortalized murine prebrown adipocyte cell line HBA cells was used for GLUT4 translocation studies [16]. Differentiated HBA cells exhibit characteristics of brown adipocytes, including expression of UCP1 and GLUT4, and respond to insulin and adrenergic stimulation [16–18,20]. Rab10 was knockdown in HBA cells by stable expression of an shRNA previously characterized in 3T3-L1 adipocytes [2]. Rab10 mRNA and protein were reduced by 80% (Figure 1A,B). Insulin-stimulated phosphorylation of Akt was not affected in Rab10 KD, demonstrating that Rab10 depletion does not disrupt insulin signal transduction (Figure 1C). To study the behavior of GLUT4, we used a dual-tagged GLUT4 reporter, HA-GLUT4-GFP, transiently expressed in HBA cells. The ratio of the anti-HA fluorescence (surface GLUT4) to GFP fluorescence (total GLUT4) reflects the proportion of GLUT4 in the plasma membrane per cell [22]. Insulin-stimulation induced an approximately 4-fold increase of GLUT4 in the plasma membrane of WT HBA cells and knockdown of Rab10 blunted the redistribution of GLUT4 to the plasma membrane by 50% (Figure 1D,E). Rab10 knockdown also blunted insulin-stimulated glucose uptake into HBA cells (Figure 1F).

To generate a model for *in vivo* studies on the role of Rab10 in primary brown adipocytes, we crossed UCP1-Cre transgenic mice to mice homozygous for loxP sites flanking exon 1 of Rab10 [3]. Rab10 protein levels were reduced in BAT-specific Rab10 knockout mouse (**bR10KO**), but unaffected in WAT, muscle, and liver, confirming the specificity of Rab10 deletion (Figure 1G).
Rab10 deletion blunted insulin-stimulated glucose uptake into BAT stromal vascular fraction-derived, *in vitro* differentiated, brown adipocytes (Figure 1H and Supplementary Figure 1). *In vitro* insulin-stimulated glucose transport was blunted in Rab10 KO *in vitro* differentiated brown adipocytes of both sexes.
These data, from two different models of brown adipocytes, establish a role for Rab10 in insulin-stimulated GLUT4 translocation and glucose uptake. These findings are in agreement with the previously documented role of Rab10 in insulin-stimulated GLUT4 translocation to the plasma membrane of white adipocytes, identifying that Rab10 is essential for the regulation of GLUT4 in adipocytes [3].

3.2. Reduced glucose tolerance and systemic insulin resistance in female, but not male bR10KO mice
Deletion of Rab10 in brown adipocytes did not affect the bodyweight nor food intake of female mice on a normal chow diet (**NCD**) (Figure 2A,B). However, bR10KO female mice were glucose intolerant with elevated plasma insulin during an intraperitoneal glucose tolerance test (**IP-GTT**) (Figure 2C representative experiment and Figure 2D–E aggregate data from multiple independent cohorts of mice). In agreement with the elevated blood insulin, bR10KO female mice were insulin resistant in an insulin tolerance test (**ITT**) (Figure 2F). Despite the impact on the metabolism of silencing Rab10 in brown adipocytes of female mice, there were no differences in whole-body fat mass, weights of individual fat depots, or histological differences of BAT and iWAT between genotypes of female mice (Figure 2G–I).
Deletion of Rab10 in brown adipocytes did not significantly change the body weight and food intake of male mice on an NCD (Figure 2J,K). IP-GTT, circulating insulin levels during an IP-GTT, and ITT were all unchanged in bR10KO male mice as compared to littermate control mice (Figures 2L–N) representative data from one cohort of mice shown, similar results in two additional cohorts studied). There were no differences in whole-body fat mass or weights of individual fat depots in male bR10KO mice compared to littermate controls (Figure 2O and P). Importantly, deletion of Rab10 from both white and brown adipocytes (adiponectin-CRE-driven deletion of Rab10 from WAT and BAT) induced whole-body insulin resistance in male mice (Figure 2Q). Thus, brown fat has a more prominent role in the whole-body regulation of female mice.

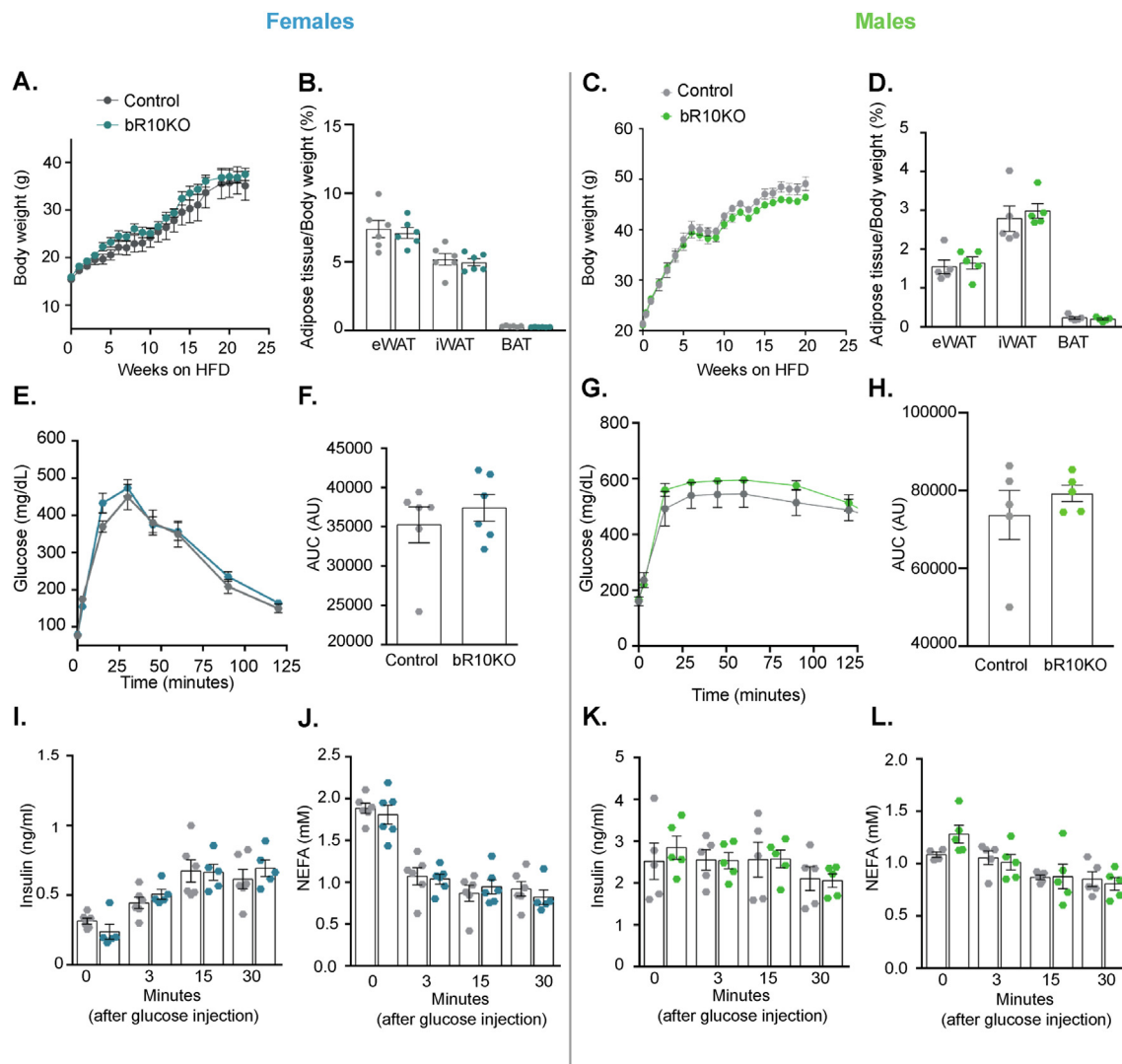### 3.3. Brown fat Rab10 knockout does not augment the metabolic impacts of a high-fat diet
Deletion of Rab10 from brown adipocytes did not affect weight gain, WAT, or BAT fat mass, in female or male mice on a high-fat diet (HFD: 20% protein, 60% fat, 20% carbohydrate) (Figure 3A–D). In addition, there were no differences within the sexes between HFD fed bR10KO and control mice in glucose tolerance, plasma insulin during a GTT, and insulin sensitivity as measured by ITT (Figures 3E-L). Thus, disruption of brown fat metabolism induced by Rab10 KO does not have additive effects on the impact of HFD on whole-body metabolism.

3.4. BAT-specific Rab10 deletion is not required to maintain body temperature with cold exposure
To test whether Rab10 deletion interferes with thermogenesis, mice were housed at 4 °C and body temperature was measured every 30 min for the first 3 h, and thereafter, once a day for 14 days (Figure 4A–D). Body temperature did not differ between control and bR10KO mice in either sex, demonstrating that the silencing of Rab10 in BAT does not affect the defense of body temperature against severe cold.
Body weight and adiposity did not differ between control and bR10KO animals in both sexes adapted to severe cold (Figure 4E–H), although there was a small (25%), albeit statistically significant decrease in BAT weight in bR10KO female mice (Figure 4F). In the BAT from bR10KO mice acclimated to severe cold, there were no changes in the mRNA expression of PRDM16 and CIDEA, whereas the levels of UCP1 and DIO2 mRNA were increased, albeit by less than 50% (Figure 4I). The small increase in UCP1 mRNA levels in bR10KO mice was not detected as in the increase in UCP1 protein expression (Figure 4J). No differences were found in UCP1, PRDM16, DIO2, or CIDEA in BAT from mice at room temperature (Figure 4I). In addition, there were no differences in the morphology of BAT between genotypes at either room temperature or with a severe cold challenge (Figure 4K and Supplementary Figure 2).
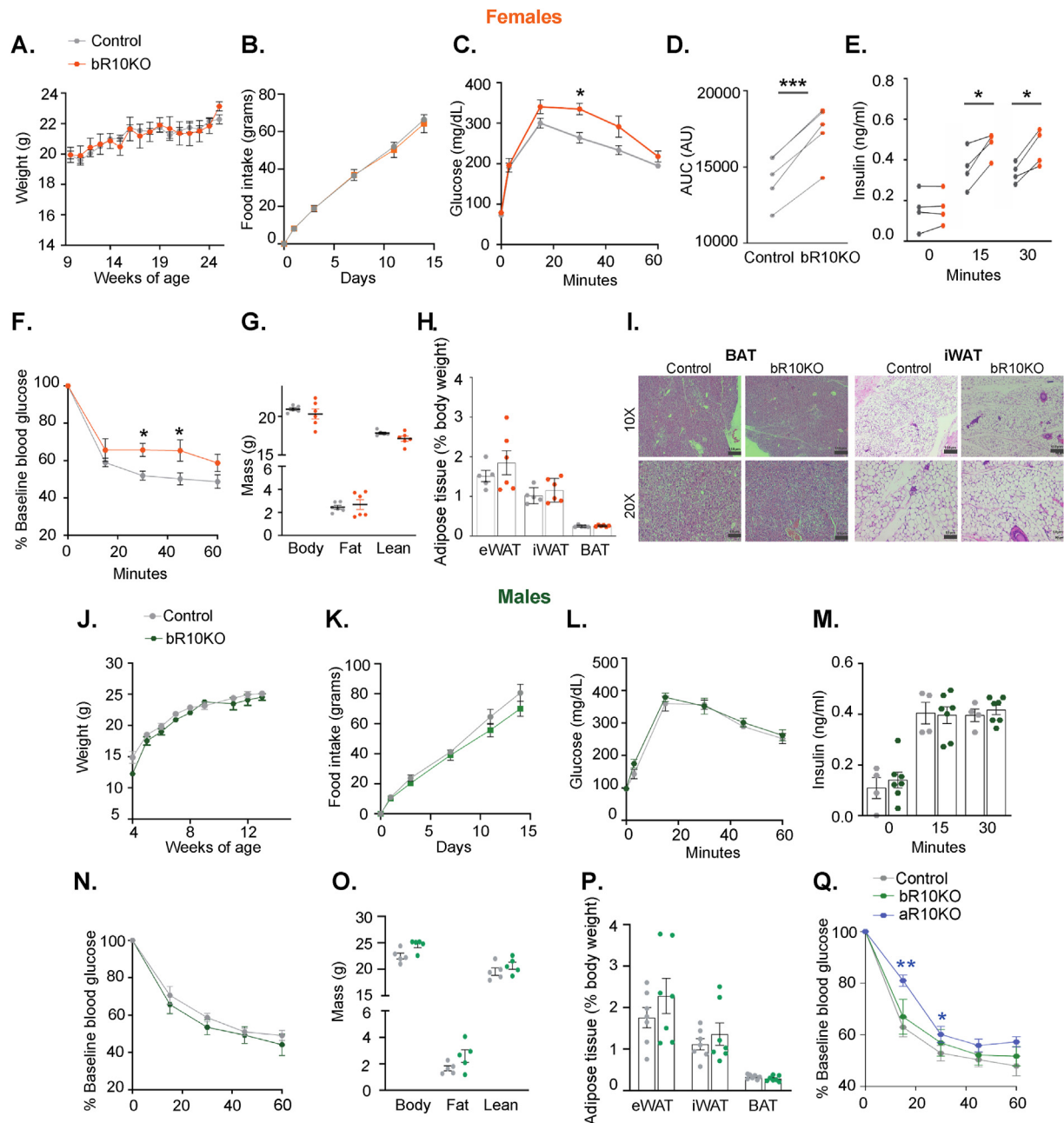
Figure 2: Loss of BAT-specific Rab10 is sufficient to induce systemic insulin resistance in chow diet-fed females, but not males. A. Bodyweight overtime in female mice (*ad libitum*) (n = 4−5 mice/group). **B.** Food intake (grams) of control and bRab10KO female mice over 14 days (n = 5 mice/group). **C.** Representative glucose tolerance test (GTT) (2 g/kg glucose intraperitoneal injection (i.p.)) in female mice aged 17 weeks (n = 4−5 mice/group). **D.** Quantification of GTT area under the curve from 5 independent cohorts of mice 17−20 weeks of age. **E.** Plasma insulin levels in female mice after overnight fasting (0 min) and 15 and 30 min after i.p. glucose injection (2 g/kg) from 4 independent cohorts of mice of 17−20 weeks of age. **F.** Representative ITT results for 17 weeks of age (0.75 unit/Kg insulin i.p). **G.** Body composition by magnetic resonance imaging (MRI) in mice aged 12 weeks (n = 6 mice/group). **H.** Adipose tissue depots weights: epididymal adipose tissue (eWAT), inguinal adipose tissue (iWAT), and brown adipose tissue (BAT) in mice aged 25 weeks (n = 5−6 mice/group). **I.** Representative H&E images of BAT and iWAT from control and bR10KO female mice. Images are shown at 10X and 20X magnification with 150 μm and 60 μm scale bars, respectively. **J.** Bodyweight overtime in male mice (ad libitum) (n = 3−5 mice/group). **K.** Food intake (grams) of control and bRab10KO male mice over 14 days (n = 5 mice/group). **L.** Representative glucose tolerance test (GTT) (2 g/kg glucose intraperitoneal injection (i.p.)) in male mice aged 17 weeks (n = 4−5 mice/group). **M.** Plasma insulin levels in male mice after overnight fasting (0 min) and 15 and 30 min after i.p. glucose injection (2 g/kg) (n = 4−7 mice/group). **N.** Representative insulin tolerance test (ITT) results for mice aged 17 weeks (0.75 unit/Kg insulin i.p.) (n = 4−6 mice/group). **O.** Body composition by MRI in mice aged 12 weeks (n = 5 mice/group). **P.** Adipose tissue depots weights: epididymal adipose tissue (eWAT), inguinal adipose tissue (iWAT), and brown adipose tissue (BAT) in mice aged 25 weeks (n = 7 mice/group). **Q.** Representative insulin tolerance test (ITT) results for mice aged 16 weeks (0.75 unit/Kg insulin i.p.) (n = 4−6 mice/group). $*p < 0.05$, $**p < 0.01$, and $***p < 0.001$.

www.molecularmetabolism.com

Females

Males

Figure 3: BAT Rab10 knockout does not augment the metabolic impacts of a high-fat diet. Female and male mice were *ad libitum* fed HFD starting at 6 weeks of age. **A.** Female mice body weight (*ad libitum*) through 17 weeks of a HFD. **B.** Adipose tissue depots weights: epididymal adipose tissue (eWAT), inguinal adipose tissue (iWAT), and brown adipose tissue (BAT) of female mice after 20 weeks of a HFD. **C.** Male mice body weight (*ad libitum*) through 25 weeks of a HFD. **D.** Adipose tissue depots weights: eWAT, iWAT, and BAT of male mice after 25 weeks of a HFD. **E.** Glucose tolerance test (GTT) (2 g/kg glucose intraperitoneal injection (i.p.)) in female mice aged 13 weeks. **F.** Quantification of GTT area under the curve (AUC). **G.** GTT (2 g/kg glucose i.p.) in male mice aged 17 weeks. **H.** Quantification of GTT area under the curve (AUC). **I.** Plasma insulin and **J.** free fatty acid levels in female mice after overnight fasting (time point 0) and 3, 15, and 30 min after i.p. glucose injection (2 g/kg). **K.** Plasma insulin and **L.** free fatty acid levels in male mice after overnight fasting (0 min) and 3, 15, and 30 min after i.p. glucose injection (2 g/kg). Female mice data n = 6 mice/group and male mice data n = 5 mice/group. Unpaired Student's t-test was used for comparing groups.

Cold challenge induces a thermogenic gene program in subcutaneous WAT, a process referred to as "browning" [23]. The morphologies of iWAT in both genotypes of mice were similarly affected by severe cold, characterized by a decrease in the size of white adipocytes and an increase in multilocular brown-like adipocytes (Figure 4L and Supplementary Figure 2). In control mice housed at 4 °C, 48% ± 2.9% of iWAT fat cells were multilocular, whereas in iWAT from bR10KO mice housed at 4 °C, 43.5% ± 9.7% of fat cells were multilocular (n = 4 mice per genotype, quantification of 5 fields per mouse). In addition, there were no differences in mRNA expressions between control and bR10KO female mice in genes upregulated in "browning" white fat (Figure 4M). Thus, iWAT from bR10KO female mice have a normal response to cold exposure, demonstrating that Rab10 deletion in brown adipocytes does not alter cold-induced WAT browning.

3.5. Thermoneutrality-adapted female bR10KO mice are insulin resistant

At thermoneutrality (30 °C for mice), loss of body heat is minimal and energy consumption for regulatory thermogenesis against cold is suppressed [24]. To better isolate the effect of Rab10 silencing on nonthermogenic functions of BAT, male and female mice were studied after adaptation to thermoneutrality for 21 days. UCP-1 driven CRE expression in BAT of mice acclimated to 30 °C was sufficient to silence Rab10 in bR10KO male and female mice (Rab10 fl/fl) (Figure 5A).

Female bR10KO mice were glucose intolerant at 30 °C, demonstrating a thermogenic-independent function of BAT in the regulation of systemic metabolism that is disrupted by Rab10 deletion in female mice (Figure 5B). There were no differences in glucose tolerance between
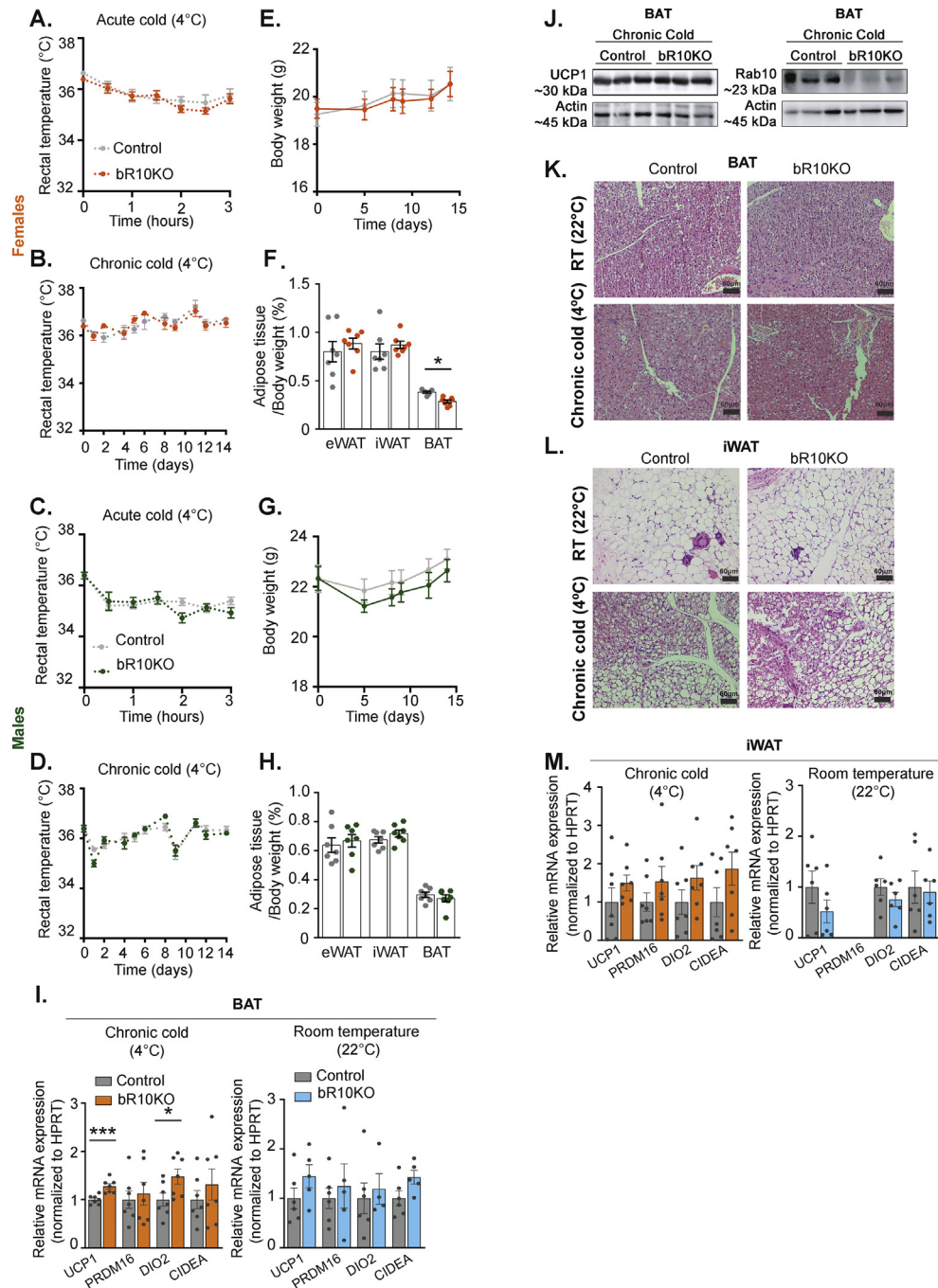
Figure 4: BAT Rab10 is not required to maintain body weight temperature when exposed to severe cold. A-D. Rectal temperature in female (**A&B**) and male (**C&D**) mice under acute (**A&C**) or chronic (**B&D**) cold (4 °C) (n = 7 mice/group). **E-H.** Bodyweight overtime (*ad libitum*) (**E&G**) and adipose tissue depots weights (**F&H**): epididymal adipose tissue (eWAT), inguinal adipose tissue (iWAT), and brown adipose tissue (BAT) of female (**E&F**) and male (**G&H**) mice after 14 days at 4 °C (n = 7 mice/group). **I.** mRNA expression for UCP1, PRDM16, DIO, and CIDEA in BAT samples of female mice housed at 22 °C (n = 4−6 mice/group) or after 14 days at 4 °C (n = 7 mice/group). **J.** UCP1, Rab10 representative immunoblots of BAT extracts from control and bR10KO mice housed at 4 °C. **K&L.** Representative H and E staining images of BAT (**K.**) and iWAT (**L.**) of mice housed at room temperature (22 °C) and chronic cold (4 °C) conditions. Images are shown at 20X magnification with 60 μm scale bars. **M.** mRNA expression for UCP1, PRDM16, DIO2, and CIDEA in iWAT samples of female mice housed at 22 °C (n = 6 mice/group) or after 14 days at 4 °C (n = 7 mice/group). Unpaired Student's t-test was used for comparing groups. *p < 0.05 and ***p < 0.001. (For interpretation of the references to color in this figure legend, the reader is referred to the Web version of this article.)

the genotypes of the male mice, re-enforcing the sex-dependence on the impact of Rab10 KO in BAT on metabolic phenotype (Figure 5C). Bodyweight and temperature did not differ between genotypes in both sexes at thermoneutrality (Figure 5D,E). Bat mass as a percent of body weight did not differ between genotypes in either

sex, and there was a similar increase in brown adipocyte size in both sexes and genotypes housed at 30 °C (Figure 5F,G and Supplementary Figure 2). There were also increases in WAT, as a percent of body weight, in both male and female bR10KO mice (Figure 5G).
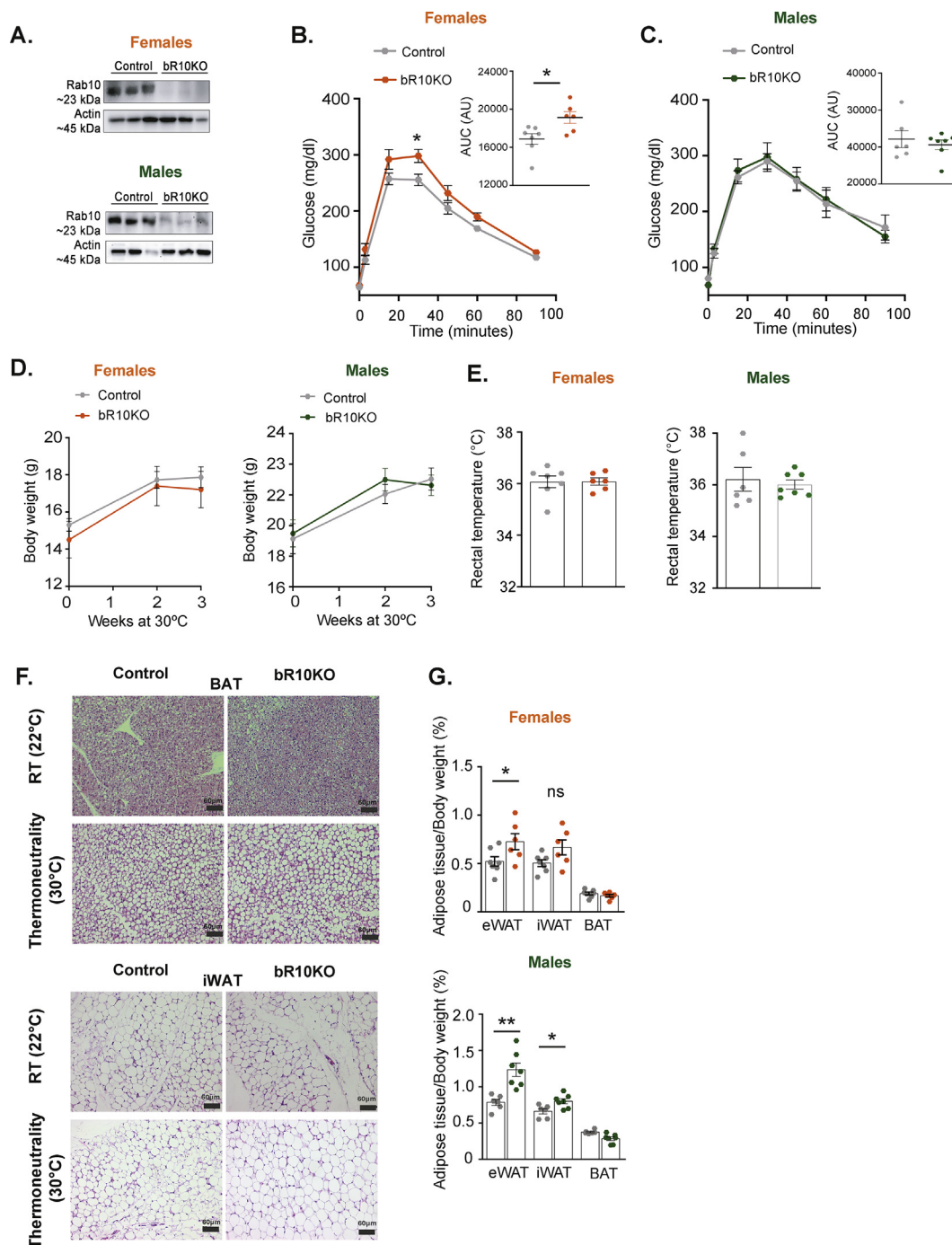
Figure 5: Thermoneutrality-adapted BRab10KO female mice are insulin resistant and both females and males have increased adiposity. A. Rab10 representative western blot of BAT extracts from control and bR10KO mice acclimated to 30 °C for 21 days. **B&C**. Glucose tolerance test (GTT) (2 g/kg glucose intraperitoneal injection (i.p.)) at day 19 of thermoneutrality acclimation in female (**B.**) and male (**C.**) mice. Inset, quantification of GTT area under the curve (AUC). n = 6−7 mice/group for all the conditions and experiments. n = 6−7 mice/group for all the conditions and experiments. **D.** Bodyweight overtime (*ad libitum*) of female and male mice at 30 °C. **E.** Rectal temperature of females and males acclimated for 21 days at 30 °C. **F.** Representative H and E staining images of BAT and iWAT from females acclimated to 22 °C or 30 °C for 3 weeks. Images are shown at 20X magnification with 60 μm scale bars. **G.** Adipose tissue depots weights: epididymal adipose tissue (eWAT), inguinal adipose tissue (iWAT), and brown adipose tissue (BAT) of female and male mice after 3 weeks at 30 °C. Unpaired Student's t-test was used for comparing groups. *p < 0.05 and **p < 0.01. (For interpretation of the references to color in this figure legend, the reader is referred to the Web version of this article).

3.6. ChREBPβ expression is reduced in Rab10KO BAT

Expression of ChREBPβ, a transcription factor involved in the regulation of lipid and glucose metabolism, is increased downstream of carbohydrate activation of ChREBPα [5]. ChREBPβ expression is reduced in bR10KO BAT of mice housed at thermoneutrality, indicating that the reduction is independent of the thermogenic activity of BAT (Figure 6A). Expression of Acc1 and FASN, two de novo lipogenesis genes and targets of ChREBPβ, are also significantly reduced

in bR10KO BAT, consistent with reduced ChREBPβ expression (Figure 6A,B). The expression of ChREBPα, the carbohydrate-sensor regulator of ChREBPβ, is not reduced in bR10KO BAT (Figure 6C). Thus, the decreased expression of ChREBPβ is likely from the reduced activation of ChREBPα, as a consequence of reduced glucose influx downstream of Rab10 silencing. Expression of SREBP1c, a transcriptional regulator of lipogenesis and glycolysis, is unchanged in bR10KO BAT (Figure 6C). Transcription of SREBP1c is increased by insulin stimulation; therefore, these data indicate that insulin signaling is intact in bR10KO brown adipocytes [25,26]. Similar changes in gene expression were observed in mice housed at room temperature (Figure 6D). Changes in the expression of genes

controlling cellular lipid homeostasis were not limited to DNL. The expression of genes involved in lipolysis, fatty acid transport, and beta-oxidation was elevated in female bR10KO BAT mice housed at thermoneutrality (Figure 6E).

Expressions of ChREBPβ and its targets, Fasn and ACC1, were not altered in the WAT of bR10KO female mice (Figure 6F). Thus, the reduced expressions of ChREBPβ and its targets are intrinsic to brown adipocytes silenced for Rab10 and not a consequence of altered whole-body metabolism of bR10KO mice. In WAT tissue of female mice, in which Rab10 is silenced in WAT (adiponectin promoter-driven CRE, aR10KO), the expressions of ChREBPβ and its targets were decreased without changes in the expressions of ChREBPα and
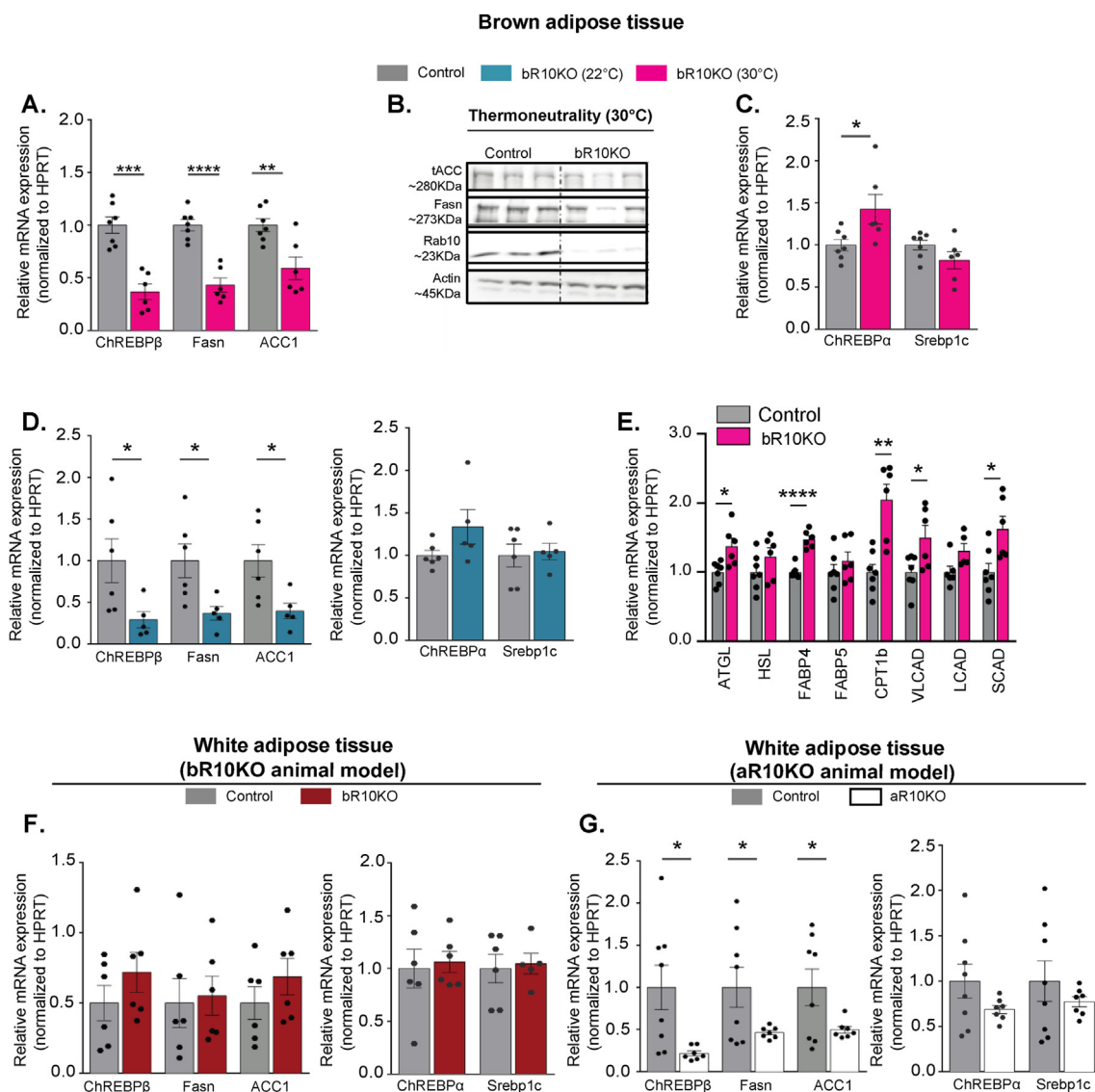
Figure 6: ChREBPβ and DNL-related gene expression are blunted in Rab10KO BAT and eWAT in a cell-intrinsic manner. A. mRNA expression for ChREBPβ, Fasn, and ACC1 in BAT samples from female mice aged 9−12 weeks at thermoneutrality (30 °C) for 3 weeks (n = 6−7 mice/group). B. Representative immunoblots of brown adipose tissue (BAT) extracts from control and bR10KO mice at 30 °C. C. mRNA expression of ChREBPα and Srebp1c in BAT samples from female mice aged 9−12 weeks at thermoneutrality (30 °C) for 3 weeks (n = 6−7 mice/group). D. mRNA expression for ChREBPβ, Fasn, ACC1, ChREBPα, and Srebp1c in BAT samples from female mice aged 9−12 weeks at room temperature (n = 5−6 mice/group). E. mRNA expression for key fatty acid transportation proteins and fatty acid lipolysis and β-oxidation enzymes in BAT samples from female mice aged 9−12 weeks acclimated to thermoneutrality (30 °C) (n = 6−7 mice/group). F&G. mRNA expression for ChREBPβ, Fasn, ACC1, ChREBPα, and Srebp1c in eWAT samples from 12 weeks of age control and bR10KO females (F.) and from 12 weeks of age control and aR10KO females (G.). Unpaired Student's t-test was used for comparing groups. *p ≤ 0.05, **p < 0.01, ***p < 0.001, and ****p < 0.0001. (For interpretation of the references to color in this figure legend, the reader is referred to the Web version of this article).

Srebp1c, reinforcing the link between decreased glucose uptake because of Rab10 silencing and reduced ChREBPβ expression (Figure 6G).

In male bR10KO mice, the expression of various DNL genes was also reduced in BAT, reinforcing the link between reduced insulin-stimulated glucose transport induced by Rab10 deletion with reduced expression of DNL genes (Supplementary Figure 3).

4. DISCUSSION

Glucose uptake by adipose tissue accounts for a small percentage (10—15%) of the disposal of a prandial glucose load [27]. Nonetheless, previous studies of mouse models with alterations in adipose insulin-regulated glucose metabolism have revealed the essential contributions of adipose glucose metabolism to systemic metabolism [3,4,28,29]. In the majority of those studies, WAT was the primary focus for understanding the link between adipose glucose metabolism and whole-body metabolic alterations. However, the adiponectin promoter-driven CRE used to generate the knockout models deletes genes from both white and brown adipocytes. Therefore, the whole-body metabolic dysregulation could result from changes in WAT and/or BAT. Here, we undertook a study of reduced insulin-stimulated glucose uptake in brown adipocytes induced by knockout of Rab10, a component of the machinery linking insulin receptor activation to GLUT4 translocation in white adipocytes [2,30,31]. Our data reveals the role of Rab10 in the regulation of GLUT4 in brown adipocytes, which contributes to BAT's function in the regulation of whole-body metabolism in female mice that is independent of the thermoregulatory function of BAT. Brown fat-specific knockout of Rab10 did not result in whole-body metabolic disruptions in male mice. These results emphasize the importance of a metabolically active BAT in whole-body glucose homeostasis in female mice, independent of thermoregulation.

4.1. Regulated glucose uptake contributes to BAT sensing nutritional states in female mice

Prior studies in male mice have established that reduced BAT mass and/or activity are associated with metabolic syndrome and obesity [32,33]. Here, we extend the understanding of BAT as a metabolic tissue by demonstrating that a partial reduction in insulin-stimulated GLUT4 translocation in brown adipocytes is sufficient to induce insulin resistance in female mice. The reduced glucose uptake is not associated with changes in BAT mass. Our results suggest that insulin-regulated glucose uptake by brown adipocytes has a role in metabolic sensing, with an approximate 50% reduction in stimulated uptake, which is sufficient to disrupt this sensing.

Rab10, in addition to its role in the regulation of GLUT4 traffic, has been described to be involved in multiple functions such as exocytosis and endosomal sorting in polarized cells [34—36]; or axonal growth in neurons [37,38]. Because Rab10 functions in the regulation of specialized membrane trafficking processes other than the regulation of GLUT4 trafficking, we cannot eliminate the possibility that Rab10 deletion in brown adipocytes, through a GLUT4-independent mechanism, contributes to changes in whole-body metabolism. However, we favor the hypothesis that it is reduced glucose uptake and metabolism in brown adipocytes, downstream of blunted GLUT4 translocation, that underlies the whole-body metabolic disruption. A previous study established that GLUT4 silencing in adipocytes (white and brown) induces systemic insulin resistance and an altered transcriptional profile of white adipocytes [4]. Knockout of Rab10 in adipocytes induces a similar systemic insulin-resistance and transcription changes as GLUT4 knockout [3]. Consequently, the most parsimonious

interpretation of the convergence of the GLUT4 and Rab10 KO models is that the effect of Rab10 knockout results from the blunted GLUT4 translocation and reduced glucose uptake.

In agreement with a role in metabolic sensing for glucose metabolism in brown adipocytes, enhanced glucose flux into brown adipocytes, induced by knockout of RalGAPB, a negative regulator of GLUT4 translocation to the plasma membrane, is associated with enhanced glucose tolerance [39,40]. Thus, brown adipocytes have a rheostat function in metabolic homeostasis, where decreased brown adipocyte glucose metabolism is associated with reduced whole-body insulin sensitivity, whereas enhanced brown adipocyte glucose metabolism is associated with improved insulin sensitivity.

4.2. CHREBPβ, a glucose sensor in brown adipocytes

ChREBP is a glucose-sensing unit critical for controlling insulin sensitivity in mice and humans [5,41]. ChREBP regulation involves direct activation of ChREBPα in response to high glucose/fructose that activates the expression of ChREBPβ, which in turn activates transcription of DNL-related genes [5]. The reduced expression of ChREBPβ, ACC1, and FASN in Rab10KO BAT female mice support ChREBP as a potential mediator of the Rab10 knockout effect. In support of a role for adipose ChREBP in determining whole-body insulin sensitivity, adipose-specific ChREBP KO is also linked to whole-body insulin resistance [7]. Although our results are in accordance with reduced BAT DNL being linked to systemic insulin resistance, genetic manipulations of adipocyte DNL report inconsistent effects with regard to systemic effects [5,42,43]. For example, the study of a tamoxifen-inducible adipose-specific FASN knockout, which blunts DNL in adipocytes, showed improved systemic glucose tolerance [44]. Disruption of the ChREBP pathway might impact the synthesis of specific lipids and/or perturb the balance of lipid species in ways distinct from the loss of FASN.

Male bR10KO mice have normal glucose tolerance and insulin sensitivity. Despite reduced expression of ChREBPβ and DNL-related genes in brown adipose tissue, female mice are permissive or male mice are dominant to the effect of Rab10 deletion from brown adipocytes. This difference is specific to BAT because deletion of Rab10 in WAT and BAT (adiponectin-CRE-aR10KO) of male mice is linked to reduced ChREBPβ expression and whole-body insulin resistance [3]. Metabolic sexual dimorphisms in mice are well known. For example, female mice demonstrate resistance to the negative metabolic consequences of a high-fat diet, although the reasons for the sexual dimorphism are not understood at present [45—47].

Furthermore, sex differences in thermogenesis have been described [48,49]. Our data extend differences between sexes in BAT function to include the impact of BAT on systemic insulin sensitivity. The reasons for differences in the impact of Rab10 deletion from brown adipocytes between male and female mice will be explored in future studies.

4.3. BAT contribution to whole-body metabolic regulation is independent of its role in thermogenesis

Glucose oxidative metabolism in BAT contributes to the fueling of nonshivering thermogenesis during cold exposure [50]. bR10KO female mice thermoregulate properly, demonstrating that the deletion of Rab10, despite disrupting whole-body metabolism, does not affect BAT's contribution to thermal regulation. Similarly, the reduced insulin-stimulated glucose uptake in BAT-specific AKT2 knockout mice is not linked to cold intolerance [51]. bR10KO female mice acclimated to thermoneutrality remain glucose intolerant and insulin resistant, providing additional evidence that the metabolic regulatory function of BAT is independent of thermogenesis. The uncoupling of BAT role in

thermogenesis from its role in the regulation of metabolism revealed by the mouse studies is in accordance with human studies demonstrating normal nonshivering thermogenesis in insulin-resistant individuals, despite reduced insulin-stimulated glucose uptake into BAT [13].

Human BAT is differently activated by insulin and cold [12]. Cold exposure increases BAT glucose uptake downstream of β-adrenergic signaling. Mechanistic studies in mouse BAT have shown that beta-adrenergic signaling stimulates glucose uptake by GLUT1-dependent and GLUT4-independent mechanism(s) [52,53]. Those data are in accordance with our findings that blunted GLUT4 translocation in BAT does not impact BAT-dependent thermogenesis.

Literature supports crosstalk between BAT and other organs that influences systemic metabolic fluxes and endocrine networks [33,54—57]. Several mechanisms have been proposed for BAT communication with other organs in the control of systemic metabolism, including protein hormones, bioactive lipids, and/or changes in innervation [7,58—60]. Additional studies are required to identify molecular mechanisms linking Rab10 knockout in brown fat to the dysregulation of whole-body metabolism in female mice. Nonetheless, we demonstrate here for the first time, the role of Rab10 on insulin-stimulated GLUT4 translocation to the plasma membrane in brown adipocytes, and we provide a unique model to understand new mechanisms of BAT function in controlling whole-body glucose metabolism.

4.4. Rab10 is required for GLUT4 translocation in brown and white adipocytes

Rab10 is required for insulin-stimulated GLUT4 translocation in white adipocytes [2], and here, we demonstrate that Rab10 is also required for GLUT4 translocation in brown adipocytes. Brown adipocytes that originate from a common precursor are shared with skeletal muscle [61]. Studies of cultured rat muscle cells have shown that the Rab8A, but not Rab10, controls muscle GLUT4 traffic in response to insulin [62]. Thus, despite the common lineage between brown adipocytes and muscle cells, adipocytes share components of the machinery that regulates GLUT4 traffic and glucose uptake, which are distinct from regulation in muscle.

5. CONCLUSIONS

Here, we demonstrate for the first time that Rab10 is required for GLUT4 translocation and glucose uptake by brown adipocytes. We provide a new mouse model which shows that the disruption of GLUT4 translocation in brown adipocytes is linked to systemic glucose homeostasis dysregulation in female mice, independent of its role in thermogenesis. Our study suggests that the reduced glucose uptake induced by Rab10 deletion disrupts ChREBP regulation of de novo lipogenesis genes in brown adipocytes. Deletion of Rab10 from male mice does not induce systemic insulin existence, although ChREBP regulation is disrupted. It is unclear whether the whole-body metabolic effects in female mice are because they are permissive to the effects of Rab10 deletion from brown adipocytes or because male mice are resistant to the effects.

AUTHOR CONTRIBUTIONS

B.P. designed and conducted experiments, analyzed the data, prepared figures, and wrote the article. L.Y. conducted experiments, analyzed the data, and edited the article. R.A.L. conducted experiments, analyzed the data, and edited the article. D.S. assisted with animal studies. E.F.J. conducted experiments and assisted with animal studies. P.C. gave advice and designed experiments. T.E.M. conceived and supervised the project, designed experiments, analyzed the data, and wrote the article.

CONFLICT OF INTEREST

None declared.

REFERENCES

[1] Klip, A., McGraw, T.E., James, D.E., 2019. Thirty sweet years of GLUT4. Journal of Biological Chemistry 294:11369—11381.

[2] Sano, H., Eguez, L., Teruel, M.N., Fukuda, M., Chuang, T.D., Chavez, J.A., et al., 2007. Rab10, a target of the AS160 Rab GAP, is required for insulin-stimulated translocation of GLUT4 to the adipocyte plasma membrane. Cell Metabolism 5:293—303.

[3] Vazirani, R.P., Verma, A., Sadacca, L.A., Buckman, M.S., Picatoste, B., Beg, M., et al., 2016. Disruption of adipose rab10-dependent insulin signaling causes hepatic insulin resistance. Diabetes 65:1577—1589.

[4] Abel, E.D., Peroni, O., Kim, J.K., Kim, Y.B., Boss, O., Hadro, E., et al., 2001. Adipose-selective targeting of the GLUT4 gene impairs insulin action in muscle and liver. Nature 409:729—733.

[5] Herman, M.A., Peroni, O.D., Villoria, J., Schön, M.R., Abumrad, N.A., Blüher, M., et al., 2012. A novel ChREBP isoform in adipose tissue regulates systemic glucose metabolism. Nature 484:333—338.

[6] Ortega-Prieto, P., Postic, C., 2019. Carbohydrate sensing through the transcription factor ChREBP. Frontiers in Genetics 10:472.

[7] Vijayakumar, A., Aryal, P., Wen, J., Syed, I., Vazirani, R.P., Moraes-Vieira, P.M., et al., 2017. Absence of carbohydrate response element binding protein in adipocytes causes systemic insulin resistance and impairs glucose transport. Cell Reports 21:1021—1035.

[8] Blondin, D.P., Carpentier, A.C., 2016. The role of BAT in cardiometabolic disorders and aging. Best Practice & Research Clinical Endocrinology & Metabolism 30:497—513.

12   MOLECULAR METABOLISM 53 (2021) 101305   www.molecularmetabolism.com

[9] Chondronikola, M., Volpi, E., Børsheim, E., Porter, C., Annamalai, P., Enerbäck, S., et al., 2014. Brown adipose tissue improves whole-body glucose homeostasis and insulin sensitivity in humans. Diabetes 63:4089—4099.

[10] Cypess, A.M., Weiner, L.S., Roberts-Toler, C., Franquet Elía, E., Kessler, S.H., Kahn, P.A., et al., 2015. Activation of human brown adipose tissue by a β3-adrenergic receptor agonist. Cell Metabolism 21:33—38.

[11] Yoneshiro, T., Aita, S., Matsushita, M., Kayahara, T., Kameya, T., Kawai, Y., et al., 2013. Recruited brown adipose tissue as an antiobesity agent in humans. Journal of Clinical Investigation 123:3404—3408.

[12] Orava, J., Nuutila, P., Lidell, M.E., Oikonen, V., Noponen, T., Viljanen, T., et al., 2011. Different metabolic responses of human brown adipose tissue to activation by cold and insulin. Cell Metabolism 14:272—279.

[13] Blondin, D.P., Labbé, S.M., Noll, C., Kunach, M., Phoenix, S., Guérin, B., et al., 2015. Selective impairment of glucose but not fatty acid or oxidative metabolism in Brown adipose tissue of subjects with type 2 diabetes. Diabetes 64: 2388—2397.

[14] Kong, X., Banks, A., Liu, T., Kazak, L., Rao, R.R., Cohen, P., et al., 2014. IRF4 is a key thermogenic transcriptional partner of PGC-1alpha. Cell 158:69—83.

[15] Kong, X., Yao, T., Zhou, P., Kazak, L., Tenen, D., Lyubetskaya, A., et al., 2018. Brown adipose tissue controls skeletal muscle function via the secretion of myostatin. Cell Metabolism 28:631—643 e633.

[16] Klein, J., Fasshauer, M., Klein, H.H., Benito, M., Kahn, C.R., 2002. Novel adipocyte lines from brown fat: a model system for the study of differentiation, energy metabolism, and insulin action. BioEssays 24:382—388.

[17] Klein, J., Fasshauer, M., Ito, M., Lowell, B.B., Benito, M., Kahn, C.R., 1999. beta(3)-adrenergic stimulation differentially inhibits insulin signaling and decreases insulin-induced glucose uptake in brown adipocytes. Journal of Biological Chemistry 274:34795—34802.

[18] Fasshauer, M., Klein, J., Kriauciunas, K.M., Ueki, K., Benito, M., Kahn, C.R., 2001a. Essential role of insulin receptor substrate 1 in differentiation of brown adipocytes. Molecular and Cellular Biology 21:319—329.

[19] Fasshauer, M., Klein, J., Neumann, S., Eszlinger, M., Paschke, R., 2001b. Tumor necrosis factor alpha is a negative regulator of resistin gene expression and secretion in 3T3-L1 adipocytes. Biochemical and Biophysical Research Communications 288:1027—1031.

[20] Fasshauer, M., Klein, J., Ueki, K., Kriauciunas, K.M., Benito, M., White, M.F., et al., 2000. Essential role of insulin receptor substrate-2 in insulin stimulation of Glut4 translocation and glucose uptake in brown adipocytes. Journal of Biological Chemistry 275:25494—25501.

[21] Klein, J., Fasshauer, M., Benito, M., Kahn, C.R., 2000. Insulin and the beta3-adrenoceptor differentially regulate uncoupling protein-1 expression. Molecular Endocrinology 14:764—773.

[22] Lampson, M.A., Racz, A., Cushman, S.W., McGraw, T.E., 2000. Demonstration of insulin-responsive trafficking of GLUT4 and vpTR in fibroblasts. Journal of Cell Science 113(Pt 22):4065—4076.

[23] Devarakonda, S., Sankararaman, S., Herzog, B.H., Gold, K.A., Waqar, S.N., Ward, J.P., et al., 2019. Circulating tumor DNA profiling in small-cell lung cancer identifies potentially targetable Alterations. Clinical Cancer Research 25:6119—6126.

[24] Lichtenbelt, W.v.M., Kingma, B., van der Lans, A., Schellen, L., 2014. Cold exposure–an approach to increasing energy expenditure in humans. Trends in Endocrinology and Metabolism 25:165—167.

[25] Foufelle, F., Ferre, P., 2007. [Unfolded protein response: its role in physiology and physiopathology]. Medical Science 23:291—296.

[26] Nadeau, K.J., Leitner, J.W., Gurerich, I., Draznin, B., 2004. Insulin regulation of sterol regulatory element-binding protein-1 expression in L-6 muscle cells and 3T3 L1 adipocytes. Journal of Biological Chemistry 279: 34380—34387.

[27] Kahn, B.B., 1996. Lilly lecture 1995. Glucose transport: pivotal step in insulin action. Diabetes 45:1644—1654.

[28] Blüher, M., Michael, M.D., Peroni, O.D., Ueki, K., Carter, N., Kahn, B.B., et al., 2002. Adipose tissue selective insulin receptor knockout protects against obesity and obesity-related glucose intolerance. Developmental Cell 3:25—38.

[29] Tanaka, N., Takahashi, S., Matsubara, T., Jiang, C., Sakamoto, W., Chanturiya, T., et al., 2015. Adipocyte-specific disruption of fat-specific protein 27 causes hepatosteatosis and insulin resistance in high-fat diet-fed mice. Journal of Biological Chemistry 290:3092—3105.

[30] Brumfield, A., Chaudhary, N., Molle, D., Wen, J., Graumann, J., McGraw, T.E., 2021. Insulin-promoted mobilization of GLUT4 from a perinuclear storage site requires RAB10. Molecular Biology of the Cell 32:57—73.

[31] Sadacca, L.A., Bruno, J., Wen, J., Xiong, W., McGraw, T.E., 2013. Specialized sorting of GLUT4 and its recruitment to the cell surface are independently regulated by distinct Rabs. Molecular Biology of the Cell 24:2544—2557.

[32] Bartelt, A., Bruns, O.T., Reimer, R., Hohenberg, H., Ittrich, H., Peldschus, K., et al., 2011. Brown adipose tissue activity controls triglyceride clearance. Nature Medicine 17:200—205.

[33] Stanford, K.I., Middelbeek, R.J., Townsend, K.L., An, D., Nygaard, E.B., Hitchcox, K.M., et al., 2013. Brown adipose tissue regulates glucose homeostasis and insulin sensitivity. Journal of Clinical Investigation 123: 215—223.

[34] Schuck, S., Gerl, M.J., Ang, A., Manninen, A., Keller, P., Mellman, I., et al., 2007. Rab10 is involved in basolateral transport in polarized Madin-Darby canine kidney cells. Traffic 8:47—60.

[35] Zou, W., Yadav, S., DeVault, L., Nung Jan, Y., Sherwood, D.R., 2015. RAB-10-Dependent membrane transport is required for dendrite arborization. PLoS Genetics 11:e1005484.

[36] Liu, O., Grant, B., 2015 Sept 22. Basolateral endocytic recycling requires RAB-10 and AMPH-1 mediated recruitment of RAB-5 GAP TBC-2 to endosomes. PLoS Genetics. https://doi.org/10.1371/journal.pgen.1005514.

[37] Liu, Y., Xu, X.H., Chen, Q., Wang, T., Deng, C.Y., Song, B.L., et al., 2013b. Myosin Vb controls biogenesis of post-Golgi Rab10 carriers during axon development. Nature Communications 4:2005.

[38] Wang, Z., Jin, Y., 2011. Genetic dissection of axon regeneration. Current Opinion in Neurobiology 21:189—196.

[39] Leto, D., Saltiel, A.R., 2012. Regulation of glucose transport by insulin: traffic control of GLUT4. Nature Reviews Molecular Cell Biology 13:383—396.

[40] Skorobogatko, Y., Dragan, M., Cordon, C., Reilly, S.M., Hung, C.W., Xia, W., et al., 2018. RalA controls glucose homeostasis by regulating glucose uptake in brown fat. Proceedings of the National Academy of Sciences of the United States of America 115:7819—7824.

[41] Baraille, F., Planchais, J., Dentin, R., Guilmeau, S., Postic, C., 2015. Integration of ChREBP-mediated glucose sensing into whole body metabolism. Physiology 30:428—437.

[42] Carvalho, E., Kotani, K., Peroni, O.D., Kahn, B.B., 2005. Adipose-specific overexpression of GLUT4 reverses insulin resistance and diabetes in mice lacking GLUT4 selectively in muscle. American Journal of Physiology. Endocrinology and Metabolism 289:E551—E561.

[43] Lodhi, I.J., Yin, L., Jensen-Urstad, A.P., Funai, K., Coleman, T., Baird, J.H., et al., 2012. Inhibiting adipose tissue lipogenesis reprograms thermogenesis and PPARgamma activation to decrease diet-induced obesity. Cell Metabolism 16:189—201.

[44] Guilherme, A., Pedersen, D.J., Henchey, E., Henriques, F.S., Danai, L.V., Shen, Y., et al., 2017. Adipocyte lipid synthesis coupled to neuronal control of thermogenic programming. Molecular Metabolism 6:781—796.

[45] Casimiro, I., Stull, N.D., Tersey, S.A., Mirmira, R.G., 2021. Phenotypic sexual dimorphism in response to dietary fat manipulation in C57BL/6J mice. Journal of Diabetic Complications 35:107795.

[46] Hwang, L.L., Wang, C.H., Li, T.L., Chang, S.D., Lin, L.C., Chen, C.P., et al., 2010. Sex differences in high-fat diet-induced obesity, metabolic alterations and learning, and synaptic plasticity deficits in mice. Obesity 18:463—469.

Original Article

[47] Peng, C., Xu, X., Li, Y., Li, X., Yang, X., Chen, H., et al., 2020. Sex-specific association between the gut microbiome and high-fat diet-induced metabolic disorders in mice. Biology of Sex Differences 11:5.

[48] Quevedo, S., Roca, P., Picó, C., Palou, A., 1998. Sex-associated differences in cold-induced UCP1 synthesis in rodent brown adipose tissue. Pflügers Archiv 436:689—695.

[49] Roca, P., Rodriguez, A.M., Oliver, P., Bonet, M.L., Quevedo, S., Picó, C., et al., 1999. Brown adipose tissue response to cafeteria diet-feeding involves induction of the UCP2 gene and is impaired in female rats as compared to males. Pflügers Archiv 438:628—634.

[50] Townsend, K.L., Tseng, Y.H., 2014. Brown fat fuel utilization and thermogenesis. Trends in Endocrinology and Metabolism 25:168—177.

[51] Sanchez-Gurmaches, J., Tang, Y., Jespersen, N.Z., Wallace, M., Martinez Calejman, C., Gujja, S., et al., 2018. Brown fat AKT2 is a cold-induced kinase that stimulates ChREBP-mediated de novo lipogenesis to optimize fuel storage and thermogenesis. Cell Metabolism 27:195—209 e196.

[52] Dallner, O.S., Chernogubova, E., Brolinson, K.A., Bengtsson, T., 2006. Beta3-adrenergic receptors stimulate glucose uptake in brown adipocytes by two mechanisms independently of glucose transporter 4 translocation. Endocrinology 147:5730—5739.

[53] Olsen, J.M., Sato, M., Dallner, O.S., Sandstrom, A.L., Pisani, D.F., Chambard, J.C., et al., 2014. Glucose uptake in brown fat cells is dependent on mTOR complex 2-promoted GLUT1 translocation. The Journal of Cell Biology 207:365—374.

[54] Liu, X., Zheng, Z., Zhu, X., Meng, M., Li, L., Shen, Y., et al., 2013a. Brown adipose tissue transplantation improves whole-body energy metabolism. Cell Research 23:851—854.

[55] Misra, A., Vikram, N.K., 2003. Clinical and pathophysiological consequences of abdominal adiposity and abdominal adipose tissue depots. Nutrition 19:457—466.

[56] Stanford, K.I., Goodyear, L.J., 2013. The therapeutic potential of brown adipose tissue. Hepatobiliary Surgery and Nutrition 2:286—287.

[57] Zhu, Z., Spicer, E.G., Gavini, C.K., Goudjo-Ako, A.J., Novak, C.M., Shi, H., 2014. Enhanced sympathetic activity in mice with brown adipose tissue transplantation (transBATation). Physiology & Behavior 125:21—29.

[58] Gunawardana, S.C., Piston, D.W., 2012. Reversal of type 1 diabetes in mice by brown adipose tissue transplant. Diabetes 61:674—682.

[59] Payab, M., Abedi, M., Foroughi Heravani, N., Hadavandkhani, M., Arabi, M., Tayanloo-Beik, A., et al., 2021. Brown adipose tissue transplantation as a novel alternative to obesity treatment: a systematic review. International Journal of Obesity 45:109—121.

[60] Yore, M.M., Syed, I., Moraes-Vieira, P.M., Zhang, T., Herman, M.A., Homan, E.A., et al., 2014. Discovery of a class of endogenous mammalian lipids with anti-diabetic and anti-inflammatory effects. Cell 159:318—332.

[61] Sanchez-Gurmaches, J., Guertin, D.A., 2014. Adipocyte lineages: tracing back the origins of fat. Biochimica et Biophysica Acta 1842:340—351.

[62] Sun, Y., Bilan, P.J., Liu, Z., Klip, A., 2010. Rab8A and Rab13 are activated by insulin and regulate GLUT4 translocation in muscle cells. Proceedings of the National Academy of Sciences of the United States of America 107:19909—19914.